# Photoelectron spectroscopy of mono-niobium carbide clusters $NbC_n^-$ ($n=2-7$): Evidence for a cyclic to linear structural transition

Hua-Jin Zhai, Shu-Rong Liu, Xi Li, and Lai-Sheng Wang[a)]
*Department of Physics, Washington State University, 2710 University Drive, Richland, Washington 99352 and W. R. Wiley Environmental Molecular Sciences Laboratory, Pacific Northwest National Laboratory, MS K8-88, P.O. Box 999, Richland, Washington 99352*

(Received 23 March 2001; accepted 29 June 2001)

We investigated a series of mono-niobium carbide clusters, $NbC_n^-$ ($n=2-7$), using anion photoelectron spectroscopy. Vibrationally resolved photoelectron spectra were observed for $NbC_2^-$ and $NbC_3^-$, which were both shown to have cyclic $C_{2v}$ structures. Two isomers were observed for $NbC_4^-$ and $NbC_5^-$. The weak and low electron binding energy isomers were shown to be cyclic structures forming a series with $NbC_2^-$ and $NbC_3^-$, and all have similar and low electron binding energies. The main isomers of $NbC_4^-$ and $NbC_5^-$, which possess much higher electron binding energies, were shown to be due to linear structures, which form a series with $NbC_6^-$ and $NbC_7^-$. All the linear $NbC_n^-$ clusters were observed to have high electron binding energies and exhibit an even–odd alternation, similar to that observed for pure linear carbon clusters in the same size range. A cyclic to linear structural transition was thus observed for the $NbC_n^-$ clusters from $NbC_3^-$ to $NbC_4^-$, with the cyclic structures favored for the smaller clusters and the linear isomers favored for the larger clusters. © *2001 American Institute of Physics.* [DOI: 10.1063/1.1395556]

## I. INTRODUCTION

Metal carbide clusters have been a fertile research area responsible for several classes of interesting clusters, including metallofullerenes,[1] metallocarbohedrenes (met-cars),[2–4] and carbide nanocrystals.[4] However, despite intensive initial research efforts to elucidate the growth mechanisms and structures of these clusters, experimental efforts in this area have leveled off. Further progress will require systematic and thorough experimental and theoretical investigations on the structure and bonding of small metal carbide clusters that will lead to detailed knowledge about the interactions between carbon and metals. One recent interesting experimental development has been the vibrational spectroscopy investigation of titanium carbide met-cars and nanocrystals using infrared multiphoton excitation.[5]

Photoelectron spectroscopy (PES) of size-selected anions is particularly powerful in providing electronic and spectroscopic information for clusters in the gas phase. We have been interested in probing the electronic structures of metal carbide clusters.[6–11] Very recently, we reported vibrationally resolved photoelectron spectra of two series of metal carbide clusters ($MC_2^-$ and $MC_3^-$) across the $3d$ series.[10,11] These results provided spectroscopic and chemical bonding information about the $3d$ $MC_2$ and $MC_3$ systems. In the current article, we report an investigation of a $4d$ mono-metal carbide cluster series, $NbC_n^-$ ($n=2-7$). Niobium interacts with carbon covalently and forms a refractory metal carbide material (NbC) in the bulk. Among the small transition metal carbide clusters, $Nb_nC_m$ are particularly interesting in that they form both met-cars and cubic nanocrystals.[12,13] It was found that formation of either met-cars or nanocrystals strongly depended on experimental conditions: the relative concentrations of the metal and carbon are believed to play a key role.[12,14] Thus, we choose $Nb_nC_m$ as a model system to investigate the formation and growth of cubic carbide nanocrystals. We have obtained PES data for $Nb_nC_m^-$ clusters with various $n$ and $m$. In the present contribution, we report on the PES results for the simplest series containing only one niobium atom, $NbC_n^-$ ($n=2-7$).

There have been a number of experimental and theoretical studies on small mono-metal carbide clusters. An early Knudsen effusion mass spectrometry study on $YC_n$ ($n=2-8$) clusters suggested that linear structures with the metal atom at one end of the carbon chain are most probable except for $YC_4$.[15] Theoretical calculations indicated, however, that small $YC_n$ clusters prefer cyclic structures, while larger clusters with $n\geqslant 6$ favor linear structures.[16] Theoretical calculations concluded that the cyclic structures are most stable for all $MC_n$ ($n=3-6$) species for M=Y and La.[17] Ion mobility experiments indicated that $LaC_n^+$ ($n=2-8$) indeed have the cyclic structures.[18] A PES study, however, suggested linear structures for all the $LaC_n^-$ ($n=2-8$) species,[19] which are in contrast to the cyclic structures suggested by the theoretical calculations for $n=2-6$.[17,20] A recent PES study on $MC_n^-$ (M=Sc, Y, and La, $n=5-20$) suggested that $MC_n^-$ clusters with odd $n$ show PES features similar to the linear carbon chains, whereas $MC_n^-$ clusters with even $n$ show PES features attributed to ring isomers.[21] A collision-induced dissociation study of $TaC_n^+$ ($n=1-14$) concluded that either a linear or a cyclic structure could be the ground state,[22] whereas a reactivity study suggested the possibility of cyclic $TaC_n^+$ structures.[23] For $FeC_n$ ($n=4-8$), an ion mobility study concluded that a linear isomer was observed for $FeC_4^-$,

a)Author to whom correspondence should be addressed. Electronic mail: ls.wang@pnl.gov

 

TABLE I. Binding energies (BE), term values, and vibrational frequencies observed from the photoelectron spectra of $NbC_2^-$ and compared to theoretical calculations (Ref. 29).

| States | BE (eV)[a] | Vib. freq. ($cm^{-1}$)[a] | Term values (exp., eV) | Term value (Theo., eV) | |
|---|---|---|---|---|---|
| | | | | B3LYP | DC-MRSDCI |
| $X^4B_1(2b_1^2 5a_1^2 1a_2^1 6a_1^1 3b_2^1)$ | 1.380 (25)[b] | 530(30) | 0.0 | 0.0 | 0.0 |
| $A^2B_1(2b_1^2 5a_1^2 1a_2^1 6a_1^1 3b_2^1)$ | 1.815 (20) | 550(40) | 0.435 | 0.41 | 0.55 |
| $B^2A_2(2b_1^2 5a_1^2 1a_2^1 6a_1^0 3b_2^2)$ | 2.155 (25) | 540(50) | 0.775 | 1.01 | 0.76 |
| $C^2A_1(2b_1^2 5a_1^2 1a_2^0 6a_1^1 3b_2^2)$ | 2.415 (25) | 560(50) | 1.035 | 1.28 | 0.80 |
| $D^4A_2(2b_1^2 5a_1^1 1a_2^1 6a_1^1 3b_2^2)$ | 2.545 (25) | | 1.165 | | |

[a]Numbers in parentheses represent uncertainties in the last digits.
[b]Adiabatic electron affinity of $NbC_2$.

and a two-dimensional isomer for $FeC_7^-$, whereas both linear and two-dimensional isomers were observed for $FeC_5^-$, $FeC_6^-$, and $FeC_8^-$.[24] Density-functional calculations on $NiC_n$ ($n=1-6$) and $Ni_2C_n$ ($n=4-6$) found that linear forms are energetically preferred for all the clusters except for $NiC_2$, $NiC_6$, and $Ni_2C_6$, which have cyclic structures.[25] These results differ from those of previous tight-binding molecular dynamics calculations.[26] Density-functional calculations on $PdC_n^+$ ($n=3-18$) and $PtC_n^+$ ($n=2-16$) revealed cyclic structures for $n=2$, linear structures for $n=3-9$, and again cyclic structures for $n>10$.[27,28]

Finally, there are several recent theoretical calculations on neutral mono-niobium carbide clusters $NbC_n$ ($n=2-8$), which concluded that, among several different kinds of structures considered, the cyclic structures are most stable (except for $n=6$, for which the linear chain is most stable), and the linear chains are the second lowest in energy.[29,30] In a previous PES study, we suggested that a possible linear-to-cyclic transition takes place for neutral $FeC_n$ clusters from $n=3$ to 4.[6] In another previous work, we reported vibrationally resolved PES data for $TiC_n^-$ ($n=2-5$), and interpreted the data using the cyclic structures.[8] Subsequent theoretical calculations confirmed the cyclic structures for $TiC_n$ ($n=2-4$) and reproduced the trend in the Ti–C stretching vibrational frequencies that we observed.[31]

In this paper, we present photoelectron spectra of mono-niobium carbide clusters $NbC_n^-$ ($n=2-7$) obtained at several photon energies. Vibrationally resolved spectra were observed for $NbC_2^-$ and $NbC_3^-$ similar to the corresponding $3d$ carbide clusters. In particular, we observed an abrupt change in the PES spectra between $NbC_3^-$ and $NbC_4^-$, which was interpreted as an indication of a cyclic-to-linear structural transition. The PES data and the trend of electron binding energies for $NbC_n^-$ ($n=4-7$) revealed striking similarity to the corresponding pure carbon clusters with one more carbon atom, $C_{n+1}^-$, suggesting that the larger $NbC_n^-$ clusters indeed possess linear structures, similar to the carbon chains.

## II. EXPERIMENT

The experiments were carried out using a magnetic-bottle time-of-flight (TOF) PES apparatus, which was described in detail elsewhere.[32] Briefly, the $Nb_nC_m^-$ anions were produced by laser vaporization of a pure niobium carbide (NbC) target. The $Nb_nC_m^-$ clusters formed in the helium carrier gas underwent a supersonic expansion through a nozzle and were skimmed to form a collimated beam. Anions were extracted from the beam at 90° into a TOF mass analyzer. Clusters of interest were selected and decelerated before crossing with a detachment laser beam from either a Q-switched Nd:YAG laser (532, 355, and 266 nm) or an ArF excimer laser (193 nm). Photoelectrons were collected at nearly 100% efficiency by the magnetic bottle and analyzed in a 3.5-m long TOF tube. Photoelectron TOF spectra were converted to electron binding energy spectra, calibrated by the known spectrum of $Rh^-$. The resolution of the electron analyzer was about $\Delta E/E \sim 2.5\%$, i.e., $\sim 25$ meV for 1 eV kinetic energy electrons.

## III. RESULTS

The PES spectra of $NbC_n^-$ ($n=2-6$) at different detachment energies are presented in Figs. 1–5, respectively. Figure 6 shows the overall PES spectral evolution with cluster size, including that of $NbC_7^-$, which was measured only at 193 nm. The PES spectra represent electronic transitions from the anions to the ground- and low-lying excited states of the neutrals. The observed detachment transitions are labeled with letters and the vertical lines represent resolved vibrational structures. The obtained electron binding energies, term values, and vibrational frequencies are summarized in Table I for $NbC_2^-$ and Table II for $NbC_n^-$ ($n=3-7$).

### A. $NbC_2^-$

The spectra of $NbC_2^-$ shown in Fig. 1 were measured at two photon energies. The 532-nm spectrum [Fig. 1(a)] revealed two well-resolved vibrational progressions. The ground-state progression ($X$) had much higher intensity with a vibrational spacing of 530 $cm^{-1}$. The 0–0 transition of the $X$ band yielded an adiabatic electron affinity (EA) of 1.380 eV for $NbC_2$. The weaker vibrational progression ($A$) represents the first excited state of $NbC_2$ and has a vibrational spacing of 550 $cm^{-1}$. The 0–0 transition at 1.815 eV for the $A$ band gave an excitation energy of 0.435 eV. The 355-nm spectrum [Fig. 1(b)] revealed more transitions beyond 2 eV binding energies. A well-resolved vibrational progression ($B$) was observed at 2.155 eV with a spacing of $\sim 540$ $cm^{-1}$. The PES features became more congested at higher binding energies. But, at least two more bands ($C$ and $D$) could be

TABLE II. Observed electron binding energies (BE), adiabatic electron affinities (EA), and spectroscopic constants for $NbC_n$ ($n=3-7$).

| | | EA (eV)[a] | BE (eV)[a,b] | Term value (eV) | Vib. freq. ($cm^{-1}$) |
|---|---|---|---|---|---|
| $NbC_3$ | *X* | 1.686 (20) | 1.686 (20) | 0 | 610 (30) |
| | *A* | | 2.535 (20) | 0.849 | 840 (50) |
| | *B* | | 2.890 (25) | 1.204 | |
| | *C* | | 3.250 (20) | 1.564 | |
| $NbC_4$ | *X* | 3.27 (7) | 3.33 (7) | 0 | |
| | *A* | | 4.34 (5) | 1.01 | |
| | *B* | | 4.97 (5) | 1.64 | |
| | *C* | | 5.24 (5) | 1.91 | |
| | *D* | | 5.42 (5) | 2.09 | |
| | *E* | | 5.63 (5) | 2.30 | |
| | *X′* | 1.93 (5) | 1.93 (5) | 0 | 480 (60) |
| $NbC_5$ | *X* | 3.54 (7) | 3.75 (7) | 0 | |
| | *A* | | 4.37 (5) | 0.62 | |
| | *B* | | 5.63 (5) | 1.88 | |
| | *X′* | 1.90 (6) | 2.00 (5) | 0 | |
| | *A′* | | 2.23 (5) | 0.23 | |
| $NbC_6$ | *X* | 3.04 (8) | 3.23 (8) | 0 | |
| | *A* | | 4.48 (5) | 1.25 | |
| | *B* | | 4.98 (5) | 1.75 | |
| $NbC_7$ | *X* | 3.82 (6) | 4.13 (6) | 0 | |
| | *A* | | 4.55 (5) | 0.42 | |
| | *B* | | 5.21 (5) | 1.08 | |
| | *C* | | 5.62 (5) | 1.49 | |

[a]Numbers in parentheses represent uncertainties in the last digits.
[b]For PES features without vibrational resolution, vertical binding energies are listed.

identified. The *C* band showed a vibrational progression with a spacing of ~560 $cm^{-1}$ and was probably overlapped with the *D* feature and the higher vibrational levels of the *B* progression. Because of the overlap with the *C* band, no vibrational features could be definitively determined for the *D* band. More congested and even weaker features existed at higher binding energies in the 355-nm spectrum. We also obtained a spectrum of $NbC_2^-$ at 266 nm, which was not shown because only weak and congested features were observed similar to the high binding energy features in the 355-nm spectrum.

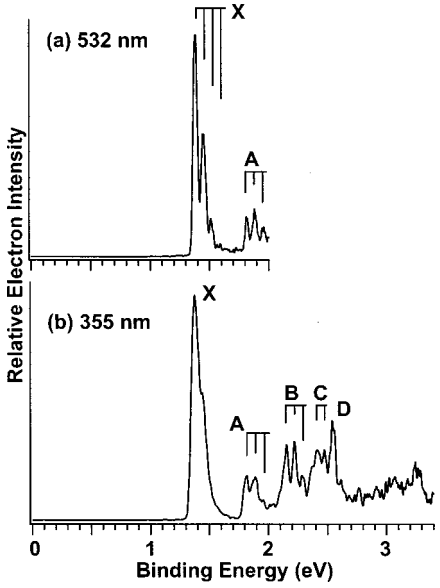


FIG. 1. Photoelectron spectra of $NbC_2^-$ at (a) 532 nm and (b) 355 nm. Vertical lines indicate vibrational structures.

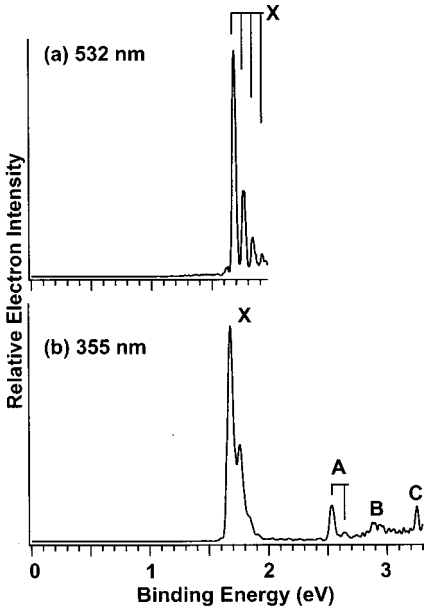


FIG. 2. Photoelectron spectra of $NbC_3^-$ at (a) 532 nm and (b) 355 nm. Vertical lines indicate vibrational structures.

### B. $NbC_3^-$

Figure 2 shows the spectra of $NbC_3^-$ at 532 and 355 nm, and they appeared to be relatively simple. The 532-nm spectrum [Fig. 2(a)] contained just one well-resolved vibrational progression (*X*) with a spacing of 610 $cm^{-1}$. The 0–0 transition defined an adiabatic EA of 1.686 eV for $NbC_3$. Three additional relatively weak bands (*A*, *B*, and *C*) were revealed at 355 nm [Fig. 2(b)]. The *A* band showed a short vibrational progression with a spacing of ~840 $cm^{-1}$ and its 0–0 transition at 2.535 eV yields an excitation energy of 0.849 eV. The *B* band was relatively broad and weak and seemed to have a not-so-well-resolved vibrational progression with an average spacing of about 580 $cm^{-1}$. A sharp peak at 3.250 eV was attributed to the 0–0 transition of a separate detachment transition (*C*). A spectrum at 266 nm was also measured for $NbC_3^-$, but was not shown since only broad and congested features were observed.

### C. $NbC_4^-$

Figure 3 shows the spectra of $NbC_4^-$ at three photon energies. Two features were observed at 355 nm [Fig. 3(a)], where the weak feature (*X′*) at 1.93 eV showed a short vibrational progression with a spacing of ~480 $cm^{-1}$, and an intense feature (*X*) at 3.33 eV appeared to be cut off at the higher binding energy side. At 266 nm [Fig. 3(b)], an even more intense band (*A*) was revealed at a vertical binding energy of 4.34 eV. Several other strong features were ob-

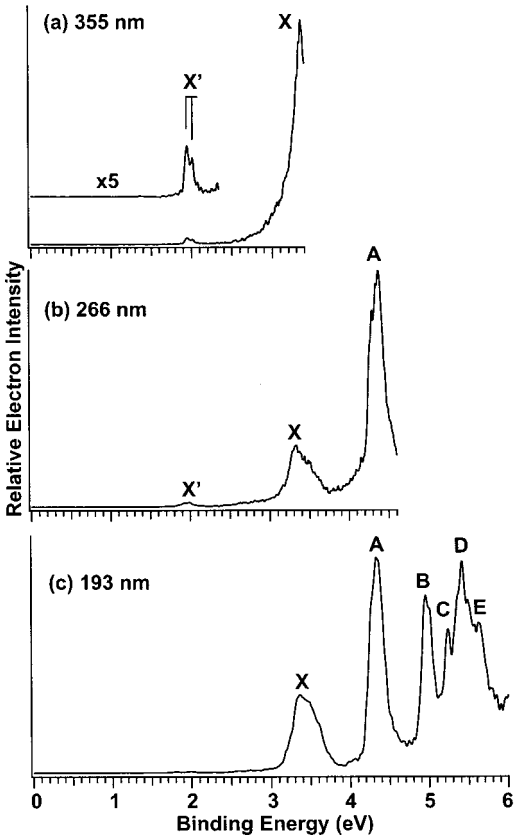


FIG. 3. Photoelectron spectra of $NbC_4^-$ at (a) 355 nm; (b) 266 nm; and (c) 193 nm. The upper trace in (a) is the enlarged 355 nm spectrum to exhibit the vibrationally resolved feature $X'$.

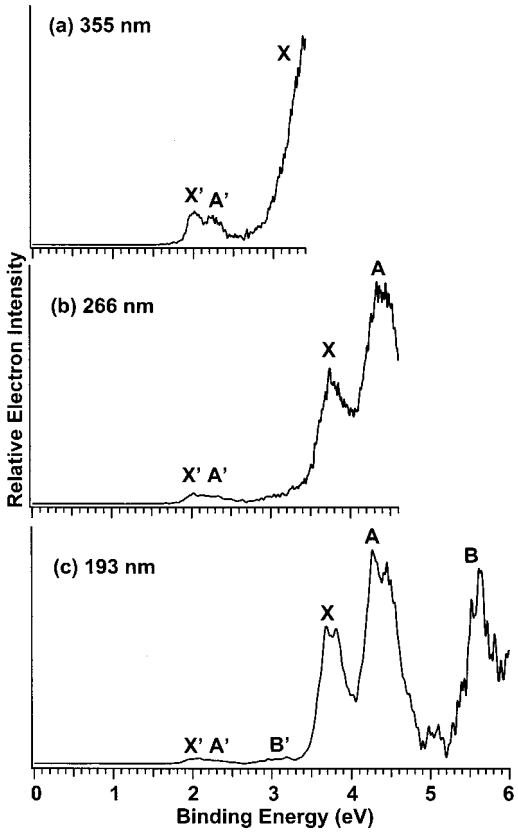


FIG. 4. Photoelectron spectra of $NbC_5^-$ at (a) 355 nm; (b) 266 nm; and (c) 193 nm.

served at 193 nm [Fig. 3(c)], including a sharp feature (*B*) at 4.97 eV and a group of congested features (*C*, *D*, and *E*).

The relative intensity of the weak feature $X'$ seemed to decrease further in the higher photon energy spectra and was no longer discernible in the 193-nm spectrum [Fig. 3(c)]. We also found that the relative intensity of the $X'$ feature depended on the source conditions to some extent, suggesting that it was likely due to a minor isomer. We could rule out the possibility of a mass contamination because our mass resolution was sufficient to resolve one atomic mass difference in this mass range (niobium has a single isotope). From the 0–0 transition of the $X'$ band we obtained an EA of 1.93 eV for the minor isomer of $NbC_4$, whereas the main *X* feature yielded an EA of 3.27 eV for the main isomer of $NbC_4$. Since no vibrational structures were resolved for the *X* band, the EA for the main isomer of $NbC_4$ was evaluated by drawing a straight line at the leading edge of the *X* band and adding a constant to the intersect with the binding energy axis to take into account of the instrumental resolution and a finite thermal effect. The features from *A* to *E* were all attributed to the main isomer of $NbC_4^-$.

### D. $NbC_5^-$

Figure 4 displays the spectra of $NbC_5^-$ at three photon energies. The 355-nm spectrum [Fig. 4(a)] exhibited two weak features ($X'$ and $A'$) and a strong high binding energy feature which was cut off. The 266-nm spectrum [Fig. 4(b)] showed that the high binding energy feature of the 355-nm spectrum was just the onset of a broadband (*X*). The 266-nm spectrum also revealed another broadband (*A*) at higher binding energies. The *X*- and *A* bands seemed to contain fine features, which were too congested to be resolved. At 193 nm [Fig. 4(c)], however, the *X*- and *A* bands were each resolved into two features, with a separation of about 960 and 1450 $cm^{-1}$, respectively. The 193-nm spectrum also showed weak features around 5 eV and an intense band (*B*) at about 5.63 eV. A weak feature ($B'$) around 3 eV appeared to be resolved at 193 nm. Again, the weak features depended slightly on the source conditions, but they could not be eliminated entirely. Similar to the weak low binding energy features in the spectra of $NbC_4^-$, we attributed the weak features ($X'$, $A'$, and $B'$) to a minor isomer of $NbC_5^-$. The weak features around 5 eV (not labeled) were likely to be from the minor isomer of $NbC_5^-$ as well. From the binding energies of the $X'$ and *X* features, we estimated the EAs to be 1.90 and 3.54 eV for the minor and major isomers of $NbC_5$, respectively (Table II).

### E. $NbC_6^-$

The spectra of $NbC_6^-$ are shown in Fig. 5 at three photon energies. The 355-nm spectrum [Fig. 5(a)] revealed one band (*X*) with partially resolved vibrational features (about 520 $cm^{-1}$ average spacing). An EA of 3.04 eV was obtained for $NbC_6$. In the 266-nm spectrum [Fig. 5(b)], one more band (*A*) was observed at higher binding energies. The *X* band at

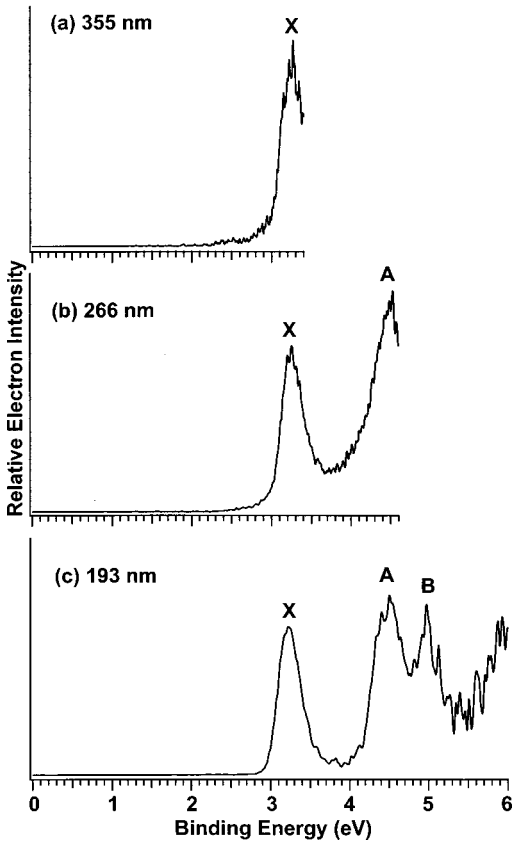


FIG. 5. Photoelectron spectra of $NbC_6^-$ at (a) 355 nm; (b) 266 nm; and (c) 193 nm.

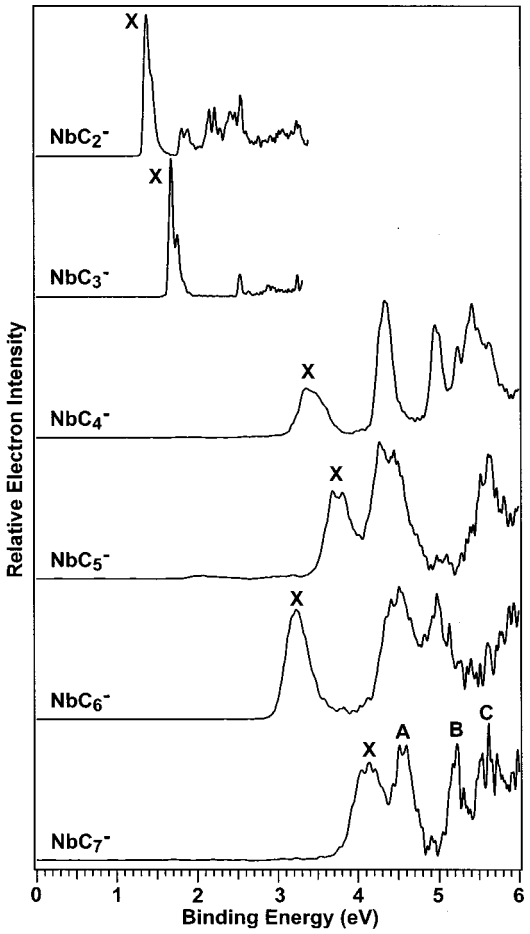


FIG. 6. Photoelectron spectrum of $NbC_7^-$ at 193 nm, compared with the spectra of the smaller clusters, $NbC_n^-$ $(n=2-6)$.

266 nm still showed partially resolved vibrational features, consistent with the 355-nm spectrum. At 193 nm [Fig. 5(c)], an additional band (*B*) and more high binding energy features were revealed, but the signal to noise ratios for these features were poor. In contrast to the spectra of $NbC_4^-$ and $NbC_5^-$, the PES spectra of $NbC_6^-$ showed no weak features at lower binding energies, indicating that there were no minor isomers present in the $NbC_6^-$ beam.

### F. $NbC_7^-$

The electron binding energies of $NbC_7^-$ were rather high and we only measured its spectrum at 193 nm, as shown in Fig. 6, where it was compared with all the other spectra of $NbC_n^-$. Four bands (*X*, *A*, *B*, and *C*) were observed, all of which showed partially resolved features. The ground-state transition (*X*) gave an EA of 3.82 eV for $NbC_7$. The binding energies of the observed features for $NbC_7^-$ are also given in Table II.

## IV. DISCUSSION

Well-resolved electronic states were observed in all the PES spectra of $NbC_n^-$, yielding a wealth of electronic structure information for the neutral $NbC_n$ clusters. Several general observations can be made immediately from the PES data. First, the EAs are low for $NbC_2$ and $NbC_3$ and increase abruptly from $NbC_3$ to $NbC_4$ (Fig. 6). Second, two distinct isomers were observed for $NbC_4^-$ (Fig. 3) and $NbC_5^-$ (Fig. 4). The minor isomers have low electron binding energies similar to that of $NbC_2^-$ and $NbC_3^-$, whereas the main isomers have much higher electron binding energies, similar to $NbC_6^-$ and $NbC_7^-$ (Fig. 6). Third, the spectra and electron binding energies of the main isomers of $NbC_n^-$ $(n=4-7)$ appeared to exhibit an even–odd alternation (Fig. 6). This even–odd alternation observed for $NbC_n^-$ was in striking analogy to that of pure carbon clusters,[34,35] as shown in Fig. 7, where the EAs of $NbC_n$ are compared to those of pure carbon clusters $(C_{n+1})$. These observations are discussed below in detail in terms of isomers and structural transitions, as well as available theoretical calculations.

### A. $NbC_2$ and $NbC_2^-$

We previously reported a systematic investigation of the $MC_2$ clusters across the first transition metal series from Sc to Co.[10] A $C_{2v}$ structure, in which the metal is side-bonded to $C_2$, was considered as the most likely candidate for $MC_2$ in interpreting the PES data. The trends of measured EAs and vibrational frequencies for the series of $MC_2$ species were found to correlate well with the corresponding monoxides (M–O), suggesting that the chemical bonding in $MC_2$ is analogous to that in M–O, i.e., the interaction between M and $C_2$ is quite ionic and $MC_2$ may be qualitatively consid-

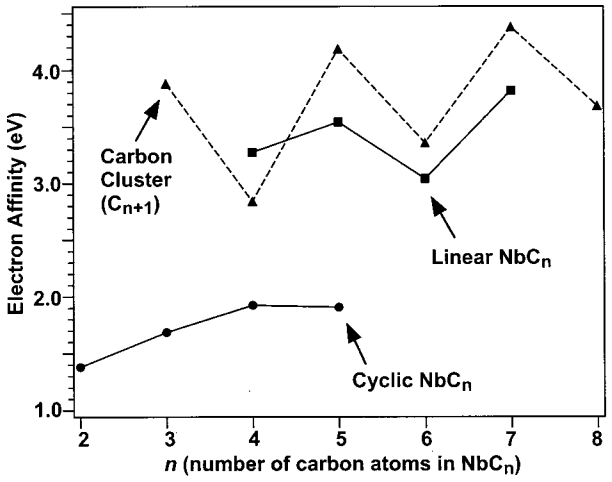


FIG. 7. The observed electron affinities (EAs) for cyclic (dots) and linear (squares) isomers of $NbC_n$ vs *n*. The EAs for the linear carbon clusters (from Ref. 35, dashed line with triangles) are also plotted for comparison. Note the similarity between the EAs of the linear $NbC_n$ clusters and the carbon clusters.

ered as $M^{2+}C_2^{2-}$ (analogous to $M^{2+}O^{2-}$). The structure and bonding of $NbC_2$ were expected to be similar to the $3d$ $MC_2$ species.

Dai *et al.* have recently performed a detailed theoretical study on the electronic structure and chemical bonding in $NbC_2$.[29] Indeed, they obtained a $C_{2v}$ structure and showed that $NbC_2$ can be viewed as $Nb^+C_2^-$ based on a large calculated dipole moment and a Mulliken population analysis. Dai *et al.* showed that the ground state of $NbC_2$ was a quartet state ($^4B_1$) and they also characterized several low-lying excited quartet, doublet, and sextet states. Based on these theoretical results, a tentative interpretation of the observed PES features is possible.

First, we compare the calculated ground-state vibrational frequencies to the experimental observation. The frequencies of the three vibrational modes calculated at the B3LYP level are: $1569\,cm^{-1}(a_1)$ for the C–C stretching, $577\,cm^{-1}(a_1)$ for the Nb–C stretching, and $301\,cm^{-1}(b_2)$ for the asymmetric mode. Our observed vibrational frequency for the ground state (*X*) is 530 $cm^{-1}$, which is in good agreement with the calculated frequency of the Nb–C stretching mode. Based on this observation, we infer that the electron removed in the photodetachment must be from an orbital primarily of Nb or Nb–C characters.

The ground state of $NbC_2$ was calculated to be a quartet $^4B_1$ state with three unpaired electrons. The valence electron configuration of the $^4B_1$ state is: $2b_1^25a_1^21a_2^16a_1^13b_2^17a_1^0$, where all the orbitals are of Nb $4d$ characters with significant mixing from C *s* and *p* orbitals and the $7a_1$ orbital is the lowest unoccupied molecular orbital (LUMO).[29] However, the $NbC_2^-$ anion was not calculated and it is not known which orbitals the extra electron would occupy in the anion ground state: it could occupy the LUMO to give a quintet ground state or enter one of the three half-filled orbitals to give a triplet ground state. Since photodetachment is primarily a one-electron process, the electron configuration of the anion ground state determines the neutral excited states that can be accessed in the PES experiment. Two-electron transitions are possible when there is significant configuration mixing in the anion ground state, though such transitions usually have much weaker cross sections.[33] Fortunately, all the electronic states calculated for $NbC_2$ are predominately of a single configuration.[29] Thus, we expected that all the PES features observed in Fig. 1 should be due to single-electron transitions. In this case, we can deduce the ground-state anion configuration based on the lowest excited state of the $NbC_2$ neutral.

The lowest excited state of $NbC_2$ calculated by Dai *et al.*[29] at the B3LYP level (0.41 eV) and the Davidson-corrected multireference (single double) configuration interaction [MR(SD)CI] level (0.55 eV) is $^2B_1$ with a configuration of $2b_1^25a_1^21a_2^16a_1^13b_2^17a_1^0$. The calculated excitation energies at the two levels of theory (given in the parentheses above) are in excellent agreement with the experimental measurement of 0.435 eV (Table I). Therefore, the anion ground state must be a triplet state and the extra electron cannot be in the $7a_1$ orbital. Based on the second calculated doublet excited state, which is $^2A_2$ with a configuration of $2b_1^25a_1^21a_2^16a_1^03b_2^27a_1^0$, we deduce that the anion ground state must be $^3A_2$ with a configuration of $2b_1^25a_1^21a_2^16a_1^13b_2^2$. The neutral states accessed through one-electron detachments from the $^3A_2$ anion are as follows:

$$2b_1^25a_1^21a_2^16a_1^13b_2^2(^3A_2)$$

$$\rightarrow 2b_1^25a_1^21a_2^16a_1^13b_2^1(^4B_1 \text{ and } ^2B_1), \quad (1)$$

$$\rightarrow 2b_1^25a_1^21a_2^16a_1^03b_2^2(^2A_2), \quad (2)$$

$$\rightarrow 2b_1^25a_1^21a_2^06a_1^13b_2^2(^2A_1), \quad (3)$$

$$\rightarrow 2b_1^25a_1^11a_2^16a_1^13b_2^2(^4A_2 \text{ and } ^2A_2). \quad (4)$$

The first three excited states from detachment channels (1)–(3) were calculated by Dai *et al.* and the calculated excitation energies are compared with the experimental values in Table I. We see that the calculated values using both methods are in reasonable agreement with the experiment. The $^4A_2$ and $^2A_2$ excited states from detachment channel (4) were not calculated. We tentatively assigned the *D* feature in the PES spectrum [Fig. 1(b)] to the $^4A_2$ state. In light of the current experimental results, it would be interesting to carry out further calculations on the anions and confirm these assignments.

### B. $NbC_3$ and $NbC_3^-$

The PES spectra of $NbC_3^-$ (Fig. 2) resembled that of $VC_3^-$.[11] A $C_{2v}$ cyclic structure was found to be the lowest in energy for the $3d$ $MC_3$ clusters from density-functional calculations, and was used to interpret the $3d$ $MC_3$ PES data.[11] Our previous PES data of $TiC_3^-$ were also interpreted using the $C_{2v}$ cyclic structure,[8] which was confirmed by subsequent theoretical calculations.[31] Considering the similarities between the PES patterns of $NbC_3^-$ and $VC_3^-$, we expected that they might possess similar $C_{2v}$ structures.

In a recent theoretical paper,[30] Dai *et al.* studied the electronic and geometrical structures of a series of mono-niobium carbide clusters, $NbC_n$ ($n=3-8$). For $NbC_3$, they

indeed obtained a $C_{2v}$ cyclic structure with a doublet ground state ($^2A_1$), which has a leading configuration of $5a_1^2 2b_1^2 4b_2^2 1a_2^2 6a_1^1$ with a $3b_1$ LUMO. The vibrational frequencies of the six modes were also calculated, though the symmetries were not designated. The 610 $cm^{-1}$ vibrational frequency observed in the PES spectra (Fig. 2) for the ground state of $NbC_3$ should be due to a symmetric Nb–C stretching mode. There are two modes with calculated frequencies (590 and 634 $cm^{-1}$) close to the experimental value, one of which should be the Nb–C stretching mode corresponding to the experimentally observed mode. It is interesting to observe that the Nb–C stretching mode has a higher frequency in $NbC_3$ than in $NbC_2$ (530 $cm^{-1}$, Table I), suggesting that the Nb–C bonding is stronger in $NbC_3$ than in $NbC_2$. This observation is also consistent with the theoretical characterizations of the chemical bonding in the cyclic $NbC_n$ clusters.[30]

A quartet ($^4B_2$) and a sextet ($^6A_1$) excited state were also calculated for $NbC_3$. According to the ground-state configuration of neutral $NbC_3$, the anion ground state can be either a singlet ($^1A_1$,$5a_1^2 2b_1^2 4b_2^2 1a_2^2 6a_1^2$) or a triplet ($^3B_1$,$5a_1^2 2b_1^2 4b_2^2 1a_2^2 6a_1^1 3b_1^1$), depending on whether the extra electron enters the HOMO($6a_1$) or the LUMO($3b_1$). If $NbC_3^-$ has the singlet ground state, only doublet excited states of $NbC_3$ can be accessed due to detachment from the fully occupied MOs. Based on the simplicity of the $NbC_3^-$ PES spectra (Fig. 2), we tentatively assigned them to be due to the closed-shell singlet $NbC_3^-$. The PES features (*X*, *A*, *B*, and *C*) were then due to removing an electron from the top four doubly occupied MOs of the $^1A_1 NbC_3^-$, respectively. On the other hand, if $NbC_3^-$ has the triplet ground state, both doublet and quartet final states can be accessed in PES, leading to more complicated spectra. We note that the calculated excitation energy of the first quartet state ($^4B_2$) is 0.98 eV above the ground state.[30] This is in good agreement with the excitation energy of the *A* feature at 0.849 eV (Table II) observed in our PES spectra. Nevertheless, the lack of calculations on the first excited doublet state prevented us from making a definitive assignment of the ground state of $NbC_3^-$.

### C. $NbC_4^-$ and $NbC_5^-$: Cyclic vs linear isomers

For $NbC_4^-$ and $NbC_5^-$, there was experimental evidence that two isomers were present in the PES spectra (Figs. 3 and 4). The minor isomers appeared to have lower electron binding energies while the main isomers have much higher electron binding energies in both $NbC_4^-$ and $NbC_5^-$. In our previous study of $TiC_n^-$, only cyclic isomers were observed. All the $TiC_n^-$ species showed relatively low and similar electron binding energies, because the extra electron occupies mainly Ti $3d$-type orbitals and the local environment of Ti in the cyclic structure is similar for different *n*. Analogously, we attributed the lower binding energy isomers of $NbC_4^-$ and $NbC_5^-$ to cyclic isomers. The magnitudes and trend of the electron binding energies for the cyclic isomers of $NbC_n^-$ ($n=2-5$) are similar to those observed for the $TiC_n^-$ clusters. The main isomers with high electron binding energies were attributed to linear isomers. We will show next that only linear isomers were observed for $NbC_6^-$ and $NbC_7^-$ and that all the linear $NbC_n^-$ isomers for $n=4-7$ form a series, analogous to pure carbon clusters with the same total number of atoms.

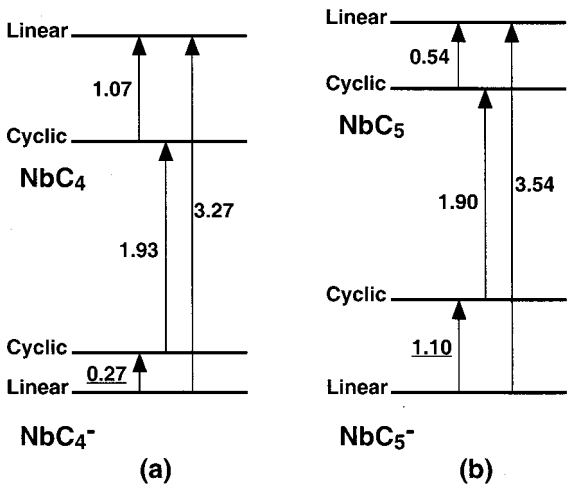


FIG. 8. Diagrams showing the energetic information and relations for the linear and cyclic isomers of (a) $NbC_4$ and $NbC_4^-$ and (b) $NbC_5$ and $NbC_5^-$. The energies are in eV. The relative energies for the neutrals are from Ref. 30. The electron affinities are from the present work (Table II).

The observation that the linear isomers dominated in $NbC_4^-$ and $NbC_5^-$ suggested that the linear anions are probably more stable than the cyclic ones. However, the recent theoretical calculations by Dai *et al.* showed that for neutral $NbC_4$ and $NbC_5$ the cyclic isomers are clearly the ground state.[30] In fact, they calculated several types of structures and spin states for the $NbC_n$ clusters at the B3LYP level of theory. For $NbC_4$, they obtained a cyclic ground state ($^4B_1$) and a low-lying quartet linear isomer, which is 1.07 eV above the $^4B_1$ ground state. For $NbC_5$, they obtained a cyclic ground state ($^2A_1$) and a low-lying quartet linear isomer only 0.54 eV above the $^2A_1$ ground state. The current data, however, showed that the linear isomers were stabilized much more in the anion states than the cyclic isomers, as revealed by the PES data in Figs. 3 and 4. Based on the neutral energetic information from Dai *et al.* and our measured adiabatic electron affinities for the cyclic and linear isomers, we estimated that the linear isomers are more stable than the cyclic isomers by 0.27 and 1.10 eV for $NbC_4^-$ and $NbC_5^-$, respectively. A schematic diagram showing the energetic information is given in Fig. 8.

All the main PES features observed for $NbC_4^-$ and $NbC_5^-$ were then attributed to the linear isomers. The spectral features were well resolved, representing the electronic excited states of the neutral linear isomers. However, without more detailed calculations on the neutral linear isomers, the spectral features could not be assigned in detail at present.

### D. $NbC_6^-$ and $NbC_7^-$: EA vs cluster size and cyclic to linear structure transition

The spectra of $NbC_6^-$ (in Fig. 5) showed no indication of low electron binding energy isomers, in contrast to those of $NbC_4^-$ and $NbC_5^-$. The spectra of $NbC_6^-$ instead appeared

similar to those of the linear $NbC_4^-$ and $NbC_5^-$ with very high electron binding energies. Dai *et al.* predicted a linear ground state for neutral $NbC_6$, but a cyclic isomer is nearly degenerate with the linear isomer and is only 0.13 eV higher in energy.[30] We thus attributed the observed PES features of $NbC_6^-$ to be due to the linear isomer. The spectrum of $NbC_7^-$ is compared with all the spectra of $NbC_n^-$ in Fig. 6. It is clear that the $NbC_7^-$ spectrum forms a series with the linear isomers of $NbC_n^-$ for $n=4-6$, all with rather high binding energies and most interestingly an even–odd alternation. The latter is revealed more clearly in Fig. 7. This even–odd alternation in electron affinities observed for the linear $NbC_n$ clusters is strikingly similar to that observed for pure carbon clusters in the same size range ($C_{n+1}$). This observation provides indirect support for the assignment of linear isomers to the $NbC_n^-$ species, since all the pure carbon clusters in this size range are known to be linear.[34,35]

Therefore, we observed a clear structural transition for the $NbC_n^-$ clusters: for $n<4$, the $NbC_n^-$ clusters prefer cyclic structures, and there is a cyclic to linear transition from $NbC_3^-$ to $NbC_4^-$. The similarity between the linear $NbC_n^-$ and pure carbon clusters is noteworthy. It suggests that the Nb atom can substitute for a carbon atom in the linear carbon clusters and form similar structures with similar electronic structures. In fact, Nb has even been observed to replace a C atom to form $NbC_n$-type of fullerene cages, again revealing the substitutional effect of Nb in $NbC_n$ clusters relative to carbon clusters.[36] Nb forms a strong covalent bond with C. The bond energy of 5.39 eV in the NbC dimer is close to the CC bond energy.[37] Thus, it is perhaps not surprising that $NbC_n^-$ clusters behave somewhat like pure $C_{n+1}^-$ clusters.

## V. CONCLUSIONS

We report a photoelectron spectroscopic investigation of mono-niobium carbide clusters, $NbC_n^-$ ($n=2-7$). Vibrationally resolved spectra were measured for $NbC_2^-$ and $NbC_3^-$, and the obtained vibrational and electronic information was compared to recent theoretical calculations. Both $NbC_2^-$ and $NbC_3^-$ were shown to have $C_{2v}$ cyclic structures and the observed Nb–C stretching vibrational frequencies were in good agreement with the theoretical results. Two distinct isomers were observed for $NbC_4^-$ and $NbC_5^-$. The weak and lower binding energy isomers were due to the cyclic structures, similar to the cyclic $NbC_3^-$, whereas the main isomers with much higher electron binding energies were shown to be due to linear isomers. $NbC_6^-$ and $NbC_7^-$ both have high binding energies and were shown to form a series with the linear isomers of $NbC_4^-$ and $NbC_5^-$. The series of linear $NbC_n^-$ clusters exhibited an even–odd alternation in electron binding energies, analogous to pure linear carbon clusters in the same size range. Thus, a cyclic to linear structure transition was observed for the $NbC_n^-$ clusters from $n=3$ to 4.

## ACKNOWLEDGMENTS

Support of this research by the National Science Foundation (No. DMR-0095828) is gratefully acknowledged. This work was performed at the W. R. Wiley Environmental Molecular Sciences Laboratory, a national scientific user facility sponsored by DOE's Office of Biological and Environmental Research and located at Pacific Northwest National Laboratory, operated for DOE by Battelle.

[1] D. S. Bethune, R. D. Johnson, J. R. Salem, M. S. de Vries, and C. S. Yannoni, Nature (London) **366**, 123 (1993); H. Shinohara, Rep. Prog. Phys. **63**, 843 (2000).
[2] B. C. Guo, K. P. Kerns, and A. W. Castleman, Jr., Science **255**, 1411 (1992); B. C. Guo, S. Wei, J. Purnell, S. Buzza, and A. W. Castleman, Jr., *ibid.* **256**, 515 (1992).
[3] M. M. Rohmer, M. Benard, and J. M. Poblet, Chem. Rev. **100**, 495 (2000).
[4] J. S. Pilgrim and M. A. Duncan, J. Am. Chem. Soc. **115**, 9724 (1993); J. S. Pilgrim and M. A. Duncan, Int. J. Mass Spectrom. Ion Processes **138**, 283 (1994).
[5] D. van Heijnsbergen, G. von Helden, M. A. Duncan, A. J. A. van Roji, and G. Meijer, Phys. Rev. Lett. **83**, 4983 (1999); G. von Helden, A. G. G. M. Tielens, D. van Heijnsbergen, M. A. Duncan, S. Hony, L. B. F. M. Waters, and G. Meijer, Science **288**, 313 (2000).
[6] L. S. Wang, Surf. Rev. Lett. **3**, 423 (1996); J. Fan and L. S. Wang, J. Phys. Chem. **98**, 11814 (1994); J. Fan, L. Lou, and L. S. Wang, J. Chem. Phys. **102**, 2701 (1995).
[7] L. S. Wang, S. Li, and H. Wu, J. Phys. Chem. **100**, 19211 (1996); L. S. Wang and H. Cheng, Phys. Rev. Lett. **78**, 2983 (1997); S. Li, H. Wu, and L. S. Wang, J. Am. Chem. Soc. **119**, 7417 (1997); L. S. Wang, X. B. Wang, H. Wu, and H. Cheng, *ibid.* **120**, 6556 (1998).
[8] X. B. Wang, C. F. Ding, and L. S. Wang, J. Phys. Chem. A **101**, 7699 (1997).
[9] X. Li, S. S. Liu, W. Chen, and L. S. Wang, J. Chem. Phys. **111**, 2464 (1999).
[10] X. Li and L. S. Wang, J. Chem. Phys. **111**, 8389 (1999).
[11] L. S. Wang and X. Li, J. Chem. Phys. **112**, 3602 (2000).
[12] S. Wei, B. C. Guo, H. T. Deng, K. Kerns, J. Purnell, S. A. Buzza, and A. W. Castleman, Jr., J. Am. Chem. Soc. **116**, 4475 (1994); J. Purnell, S. Wei, and A. W. Castleman, Jr., Chem. Phys. Lett. **229**, 105 (1994).
[13] J. S. Pilgrim, L. R. Brock, and M. A. Duncan, J. Phys. Chem. **99**, 544 (1995).
[14] B. V. Reddy and S. N. Khanna, Chem. Phys. Lett. **209**, 104 (1993).
[15] M. Pelino, R. Haque, L. Bencivenni, and K. A. Gingerich, J. Chem. Phys. **88**, 6534 (1988).
[16] S. Roszak and K. Balasubramanian, J. Phys. Chem. **100**, 8254 (1996).
[17] D. L. Strout and M. B. Hall, J. Phys. Chem. **100**, 18007 (1996).
[18] K. B. Shelimov, D. E. Clemmer, and M. F. Jarrold, J. Phys. Chem. **99**, 11376 (1995).
[19] S. Suzuki, M. Kohno, H. Shiromaru, Y. Achiba, H. Keitzmann, B. Kessler, G. Gantefor, and W. Eberhardt, Z. Phys. D: At., Mol. Clusters **40**, 407 (1997).
[20] S. Roszak and K. Balasubramanian, J. Chem. Phys. **106**, 158 (1997).
[21] M. Kohno, S. Suzuki, H. Shiromaru, K. Kobayashi, S. Nagase, Y. Achiba, H. Kietzmann, B. Kessler, G. Gantefor, and W. Eberhardt, J. Electron Spectrosc. **112**, 163 (2000).
[22] S. W. McElvany and C. J. Cassady, J. Phys. Chem. **94**, 2057 (1990).
[23] C. J. Cassady and S. W. McElvany, J. Am. Chem. Soc. **112**, 4788 (1990).
[24] G. von Helden, N. G. Gotts, P. Maitre, and M. T. Bowers, Chem. Phys. Lett. **227**, 601 (1994).
[25] C. Rey, M. M. G. Alemany, O. Dieguez, and L. J. Gallego, Phys. Rev. B **62**, 12640 (2000).
[26] A. N. Andriotis, M. Menon, G. E. Froudakis, and J. E. Lowther, Chem. Phys. Lett. **301**, 503 (1999).
[27] D. L. Strout, T. F. Miller III, and M. B. Hall, J. Phys. Chem. A **102**, 6307 (1998).
[28] T. F. Miller III and M. B. Hall, J. Am. Chem. Soc. **121**, 7389 (1999).
[29] D. Dai, S. Roszak, and K. Balasubramanian, J. Phys. Chem. A **104**, 5861 (2000).
[30] D. Dai, S. Roszak, and K. Balasubramanian, J. Phys. Chem. A **104**, 9760 (2000).
[31] R. Sumathi and M. Hendrickx, J. Phys. Chem. A **102**, 4883 (1998); R. Sumathi and M. Hendrickx, Chem. Phys. Lett. **287**, 496 (1998).
[32] L. S. Wang, H. S. Cheng, and J. Fan, J. Chem. Phys. **102**, 9480 (1995); L. S. Wang and H. Wu, in *Advances in Metal and Semiconductor Clusters, Vol. 4, Cluster Materials*, edited by M. A. Duncan (JAI, Greenwich, 1998), pp. 299–343.

[33] S. Suzer, S. T. Lee, and D. A. Shirley, Phys. Rev. A **13**, 1842 (1976).
[34] S. Yang, K. J. Taylor, M. J. Craycraft, J. Conceicao, C. L. Pettiette, O. Cheshnovsky, and R. E. Smalley, Chem. Phys. Lett. **144**, 431 (1988).
[35] D. W. Arnold, S. E. Bradforth, T. N. Kitsopoulos, and D. M. Neumark, J. Chem. Phys. **95**, 8753 (1991).
[36] D. E. Clemmer, J. M. Hunter, K. B. Shelimov, and M. F. Jarrold, Nature (London) **372**, 248 (1994); D. E. Clemmer and M. F. Jarrold, J. Am. Chem. Soc. **117**, 8841 (1995).
[37] B. Simard, P. I. Presunka, H. P. Loock, A. Berces, and O. Launila, J. Chem. Phys. **107**, 307 (1997).